Determination of Neutron Flux Parameters after Installation of Cd-Lined for Implementations of ENAA and FNAA with NIRR-1

R.L. Njinga
Physics Department
Ibrahim Badamasi Babangida University
Lapai, Niger State
Nigeria

Y.V. Ibrahim
Center for Energy Research and Training
Ahmadu Bello University
Zaria, Nigeria

M.O. Adeleye
African Leadership Academy
Johannesburg, South Africa

S.A. Jonah
Center for Energy Research and Training
Ahmadu Bello University
Zaria, Nigeria

Abstract

A permanent Cd-lined irradiation channel has been installed in one of the large outer channel of NIRR-1 for use in epithermal and fast NAA procedures. Measurements performed with Cu-wires and (0.1)%Au-Al foils to characterize the thermal, epithermal column and check its effect on the neutron flux distributions via the specific activities obtained using (n,γ), (n,p) and (n,α) reactions in other channels (A-1, B-2, B-3, and B-4) shows that the flux distributions have not been affected by the Cd-liner in outer channel A-3. The epithermal neutron flux and fast neutron flux in the Cd-lined Channel A-3 were determined using 0.1%Au-Al foil monitor via the $^{197}Au(n, \gamma)^{198}Au$ and $^{27}Al(n, p)^{27}Mg$ reactions and results were 3.96E+09 $ncm^{-2}s^{-1}$ and 1E+10$ncm^{-2}s^{-1}$ respectively at an operating power of 15.5kW which correspond to a thermal neutron flux setting of 5.0E+11$ncm^{-2}s^{-1}$ on the control console. The thermal flux evaluation was 4.89E+11$ncm^{-2}s^{-1}$ in the inner channels A-1, B-2, B-3 and 2.45E+11$ncm^{-2}s^{-1}$ in the outer channel B-4. The epithermal flux in the inner channels was 2.55E+10$ncm^{-2}s^{-1}$ and 1.28E+11$ncm^{-2}s^{-1}$ in the outer B-4. The epithermal and fast neutron flux in the Cd-lined channel provides a platform for implementation of epithermal and fast NAA techniques in NIRR-1.

Keywords: NIRR-1, Cd-lined channel, neuron flux, and flux characterization

1. Introduction

The first and only Miniature Neutron Source Reactor (MNSR) in Nigeria called NIRR-1 was designed by the China Institute of Atomic Energy (CIAE) (Zhou Yongmao, 1986). This reactor achieved first criticality on 03 February 2004 and has been operated safely till date (Jonah *et al.,* 2005; 2006). This reactor however, was specifically designed for use in Neutron Activation Analysis (NAA) and limited radioisotope production (Balogun *et al.,* 2005). The reactor (NIRR-1) has a tank-in-pool structural configuration and a core of 230 x 230 mm square cylinder fueled by U-Al4 enriched to 90% in Al-alloy cladding. It has a total number of 347 fuel pins and three Al dummies in the fuel lattice and a nominal thermal power rating of 31 kW. The length of the fuel element is 248 mm meanwhile the active length is 230 mm with 9 mm Al-alloy plug at each end (Jonah *et al.,* 2006). The reactor (NIRR-1) is basically functioning with only one Control Rod serving as shim rod, regulation rod as well as safety rod.

The startup, steady-state operation, and shutdown of the reactor are accomplished by moving the control rod which is made up of Cd absorber of about 266 mm long and 3.9 mm in diameter with stainless steel of 0.5 mm thickness as the cladding material (Jonah *et al.,* 2006). NIRR-1 is operated using the control console, the micro computer control system and the two rabbit systems all connected to a power source and during normal operation the reactor water temperature varies between 23°C and 46°C. However, the temperature difference rises rapidly and attains a stable value due to the 'insufficient natural circulation' phenomenon. One basic feature of NIRR-1 (similar facilities) is the inherent safety due to limited core excess reactivity designed to be less than ½βeff and large negative total temperature coefficient of reactivity. This feature of NIRR-1 limits the operation time for full power to 4½ hours maximally (Jonah *et al.,* 2007). NIRR-1 was acquired for elemental analysis by NAA method. On the basis of the neutron spectrum characteristics in the irradiation channels, two regimes of irradiation depending on the half-life of product radionuclide have been adopted. For the analysis of elements via very short-lived nuclides in seconds the regime is called S1 and is recommended in conjunction with Rabbit Type B. Generally, for multi-element determination, the irradiation and counting regimes S2 and S3 are specified in Table 1.

For the analysis of basic food diets and some major elements as shown in Table 1, irradiations are performed in any of the outer channels to minimize nuclear interference. Irradiations are also performed in any of the inner channels for important elements as shown in Table 1.

Table 1: Irradiation and Counting Regimes Adopted for Routine Analysis with NIRR-1 Facility

Neutron flux	Irradiation time (T_{irr})	Delayed time (T_d)	Measurement time (T_m)	Element of interest.
8.10 E+11 $ncm^{-2}s^{-1}$ NAA, B-1 3-5 cycles	30-60s	3-5s	40-60s	Se, F, Rb, O, Sc
2.25E+11 $ncm^{-2}s^{-1}$ Outer irradiation channels B-4,A-3	2-10m	1-10m 3-5h	5-10m 5-10m	Al, Mg, Cl, Ca, Cu, Ti, V, Br, Sr, I, S Na, K, Dy, Mn,
5.0E+11 $ncm^{-2}s^{-1}$ Inner irradiation channels B-2, B-3, and A-1	6-7h	2-3d,	20-30m	Na, K, As, Zn, Sb,Dy Br, Mo, La, Sm, Au, W, Ho, U, Ga, Lu, Ba, Yb
		10-15d	60m	Sc, Ce, Co, Cr, Cs Eu, Gd, Lu, Ba, Mo, Nd, Rb, Sb, Se, Ta, Tb, Th, Yb, Zn, Cd, Fe, Sr, Ag, Hf, Ir, Hg, Zr, Te, Os

Thus, careful and complete characterization of the neutron flux parameters in the irradiation channels in order to optimize its operation for NAA via relative, absolute and single comparator methods are basically very necessary as aimed in this paper after a permanent Cd-liner was installed in A-3 outer irradiation channel. The cross sectional view of NIRR-1 showing all the channel locations has been shown in a published work by Jonah *et al.*, (2004). As aimed in this work, the neutron flux spectrum parameters such as thermal flux $\left(\Phi_{th}\right)$ epithermal flux $\left(\Phi_{epi}\right)$ and fast flux $\left(\Phi_{fast}\right)$ measurements are vital in the k_0-standardization method in neutron activation analysis (NAA) and fast neutron activation analysis (De Corte, 1992, 1994, 2001). The specific activity ratio measurements with respect to the (n, γ), (n, p), (n, α) reactions in NIRR-1 irradiation channels; A-1, A-3, B-2, B-3, and B-45 to ascertain neutron flux stability measurements after the recent Cd-lined installation in A-3 was evaluated. This was aimed to assess the extent of neutron fluxes perturbation caused by the installation. The Cd-lined installation in A-3 is basically targeted toward the use of epithermal neutrons for (n, γ) reactions and fast neutrons for threshold nuclear reactions involving the ejection of more than one nuclear particles such as (n,p), (n,α), and (n,2n) and typical examples includes; $^{16}O(n,p)^{16}N$, $^{14}N(n, 2n)^{13}N$, $^{29}Si(n,p)^{29}Al$, $^{27}Al(n,p)^{27}Mg$ and $^{27}Al(n,\alpha)^{24}Na$ (Yavar *et al.,* 2011).

Generally, fast neutrons are essential in detection of metal contamination in soil, analysis of oxygen content in a wide variety of matrices including geologic materials, coal, liquid fuels, ceramic materials, petroleum derivatives, and fractions and chemical reaction products. The determination of nitrogen content in biological materials as an indication of protein content and the determination of nitrogen content of fertilizers, explosives, and polymers are also important applications. Other elements that are routinely analyzed by fast neutrons include Ag, Al, Au, Si, P, F, Cu, Mg, Mn, Fe, Zn, As, and Sn (Witkowska *et al*., 2005).

2. Theory

For the fact that detected peak intensities of irradiated samples under investigation depend solely on the induced activities, specific intensity A_{sp} are obtained from the relation below:

$$A_{sp} = \left(\phi_{th}\sigma_{th} + \phi_{ep}I_0\right)\frac{N_{av}}{M}P_i f_\gamma \varepsilon_p = \frac{N_p/t_m}{SDCm} \qquad (1)$$

Thus, for irradiation channels; A-1, B-2, B-3, and B-4 we employed $A_{bare} = \dfrac{N_p/t_m}{SDCm}$,while for the Cd-lined channel A-3 we used $A_{Cd-lined} = \dfrac{\left(N_p\right)_{Cd}/t_m}{SDCm}$, where A_{bare} = activity of non shield monitored foils and, A_{Cd} = activity of Cd-lined channel of monitored foils, S = saturated factor $\left(1-e^{\lambda t_i}\right)$, D = decay factor $\left(e^{-\lambda t_d}\right)$, C = counting factor $\left(\dfrac{1-e^{-\lambda t_m}}{\lambda t_m}\right)$, m = mass of the monitored foils. The cadmium ratio method in which a set of N=3 monitors (^{197}Au – ^{96}Zr – ^{94}Zr) were irradiated with and without Cd cover in the inner and outer irradiation channels; A-1, B-2, B-3 and B-4, and the induced activities were obtained using Eq. 1. Due to the fact that all used monitors flux obeyed the $\sigma(v)$ versus 1/v dependance concept, and by means of an iterative procedure for the set of N=3 monitors, $\log\dfrac{\overline{E}_{r,i}^{-\alpha}}{\left(F_{Cd}.R_{Cd,i}-1\right)Q_{0,i}\left(\alpha\right)\dfrac{G_{e,i}}{G_{th,i}}}$ can be written as Eq. 2 and α value obtained as the root of the equation (Jonah *et al*., 2005):

$$\alpha + \frac{\sum_{i=1}^{N}\left[\left(\log\overline{E}r,i - \dfrac{\sum_{i=1}^{N}\log\overline{E}r,i}{N}\right).\left(\log\dfrac{\overline{E}r,i^{-\alpha}}{\left(F_{Cd}.R_{Cd,i}-1\right)Q_{0,i}(\alpha)G_{e,i}/G_{th,i}} - \dfrac{\sum_{i=1}^{N}\log\dfrac{\overline{E}r,i^{-\alpha}}{\left(F_{Cd}.R_{Cd,i}-1\right)Q_{0,i}(\alpha)G_{e,i}/G_{th,i}}}{N}\right)\right]}{\left(\sum_{i=1}^{N}\log\overline{E}r,i - \dfrac{\sum_{i=1}^{N}\log\overline{E}r,i}{N}\right)^2} = 0 \qquad (2)$$

where $Q_0\left(\alpha\right) = \dfrac{I_0\left(\alpha\right)}{\sigma_{th}} = \dfrac{Q_0 - 0.429E_a^\alpha}{\overline{E}_r^\alpha} + \dfrac{0.429E_a^\alpha}{\left(2\alpha+1\right)E_{Cd}^\alpha}$ and $Q_{o,i} = I_0/\sigma_0$ is the ratio of resonance integral to thermal neutron capture cross section at neutron velocity of 2200m/s for the *i*th monitor and *i* denotes the *i*th monitor, *N* the number of monitor used, F_{Cd} is the Cd-transmission factor for epithermal neutrons; F_{Cd} (^{198}Au) = 0.991 , $G_{e,i}$ is the epithermal neutron self shielding factor for the *i*th monitor; $G_{e,i}$ (^{95}Zr) = 0.983, $G_{th,i}$ is the thermal neutron self shielding factor for the *i*th monitor, $I_0\left(\alpha\right)$ is the modified resonance integral, $\overline{E}_r^\alpha$ is the effective resonance energy (eV), $E_a^\alpha = 1^\alpha$ is the 1eV arbitrary energy and $E_{Cd}^\alpha = 0.55^\alpha$ is the effective cadmium cutoff energy.

The flux ratios (*f*) in NIRR-1 are obtained from experimentally determined cadmium ratio using the induced activity method in Eq.1. Thus, the experimental equation used in obtaining the activity ratio R_{Cd} using Eq.1 was as follows:

$$R_{Cd} = \frac{A_{bare}}{F_{Cd} A_{Cd}} = \frac{R}{R_{epi}} = \frac{\left(\Phi_{th}\sigma_{th} + \Phi_{epi} I_0\right)}{\Phi_{epi} I_0} \quad (3)$$

where F_{Cd} = cadmium transmission factor

Simplifying Eq. (3) yield

$$\left(R_{Cd} - 1\right) = \left(\frac{\Phi_{th}}{\Phi_{epi}}\right)\left(\frac{\sigma_{th}}{I_0}\right) \quad (4)$$

where $\frac{\Phi_{th}}{\Phi_{epi}}$ is defined as the thermal to epithermal flux ratio f and $\frac{I_o}{\sigma_{th}}$ is defined as the resonance integral to thermal cross-section ratio Q_0.

Hence, from Eq. 4 the thermal to epithermal ratio of the irradiation channels were obtained as;

$$f = \left(R_{Cd} - 1\right) Q_0 = \frac{\Phi_{th}}{\Phi_{epi}} \quad (5)$$

From Eq. (5), it became obvious that the neutron flux ratio (*f*) is a factor of only two parameters Q_0 and R_{Cd}.

The monitors fluxes $^{197}Au,_a$ and $^{94}Zr,_b$ were irradiated in the inner and outer irradiation channels; A-1, B-2, B-3, and B-4 of NIRR-1 under uniform neutron distribution and making use of Eq. (4) we obtained:

$$\left(R_{Cd} - 1\right)_{(a)} Q_0(\alpha)_{(a)} = \left(R_{Cd} - 1\right)_{(b)} Q_0(\alpha)_{(b)} \quad (6)$$

Putting the value of $Q_0(\alpha)$ into Eq. (6) and rearranged yield:

$$\frac{\left(R_{Cd} - 1\right)_{(a)}}{\left(R_{Cd} - 1\right)_{(b)}} = \frac{Q_b(\alpha)}{Q_a(\alpha)} = f(\alpha) \quad (7)$$

where the subscripts 'a' and 'b' represent ^{197}Au and ^{94}Zr respectively.

In measurement of the epithermal neutron spectrum flux measurement, the correction of resonance integrals I_0 to $I_0(\alpha)$ values given as $I_0(\alpha) = \left(\frac{I_0 - 0.429\sigma_{th}}{E_r} + \frac{0.429\sigma_{th}}{(2\alpha+1)E_{Cd}^{\alpha}}\right)E_a^{\alpha}$ was done and the equation use was given as (De Corte *et al.,* 2005);

$$\Phi_{epi} = \frac{N_p \lambda M}{S \times D \times \left(1 - e^{-\lambda t_m}\right) \times I_0(\alpha) \times \theta \times I_\lambda \times N_A \times w \times \varepsilon_p \times c} \quad (8)$$

The nuclear reactions employed in the evaluation of epithermal neutron spectrum flux measurement using Eq. 8 are shown below;

1. $^{65}Cu(n, \gamma)^{66}Cu$ (1039 keV, 511keV; $T_{1/2}$=5mins)
2. $^{63}Cu(n, \gamma)^{64}Cu$ (1346 keV; $T_{1/2}$=12.7hrs)
3. $^{197}Au(n, \gamma)^{198}Au$ (411.80 keV; $T_{1/2}$=2.7days)

For the measurement of the thermal neutron spectrum flux parameter, the correction of thermal to neutron cross section Q_0 to $Q_0(\alpha)$ values given as $Q_0(\alpha)=\frac{I_0(\alpha)}{\sigma_{th}}=\frac{Q_0-0.429E_a^{\alpha}}{\overline{E}_r^{\alpha}}+\frac{0.429E_a^{\alpha}}{(2\alpha+1)E_{Cd}^{\alpha}}$ was used. The Φ_{th} flux was evaluated as;

$$\Phi_{th}=\frac{N_p\lambda M}{S\times D\times\left(1-e^{-\lambda t_m}\right)\times\sigma_{th}\left(1+\frac{Q_0(\alpha)}{f}\right)\times\theta\times I_\lambda\times N_A\times w\times\varepsilon_p\times c} \quad (9)$$

The nuclear reactions employed for this measurement were 1, 2, and 3 above.

For the fast neutron flux measurements, the average cross section values were used and the Φ_{fast} measurement was obtained as follows;

$$\Phi_{fast}=\frac{N_p\lambda M}{S\times D\times\left(1-e^{-\lambda t_m}\right)\times\bar{\sigma}_f\times\theta\times I_\lambda\times N_A\times w\times\varepsilon_p\times c} \quad (10)$$

The nuclear reactions employed for this measurement were;

4. $^{27}Al(n, p)^{27}Mg$ (1014 keV, 843 keV; $T_{1/2}$=9.46mins)
5. $^{27}Al(n, \alpha)^{24}Na$ (1368.6 keV, $T_{1/2}$=14.96hrs)

where θ = isotopic abundance, λ = decay constant= $=\ln 2/T_{1/2}$, c= concentration of foil monitor, ε_p = peak efficiency, I_λ = gamma abundance, w=weight of foil monitor, t_{irr} = irradiation time, t_c = cooling time after irradiation, t_m = measuring time, $\bar{\sigma}_f$ =average cross section for fast neutron, M=atomic weight, N_A =Avogadro's number, N_p = net peak area.

3. Experimental

The Φ_{fast}, Φ_{th}, and Φ_{epi} for the two irradiation channels A-3, B-2, were measured at a neutron thermal flux rate of 5.0E+11 n/cm^{2}s in the inner channels and 2.5 E+11 n/cm^{2}s in the outer channels. The vials were of 1mm wall thickness, 1 cm diameter, and 3cm length used for inner irradiations channels while 1mm wall thickness, 2.5 cm diameter, and 3 cm length for outer irradiation channels. Two monitors made of 0.1% Au-Al foil alloy; 0.1 mm thick, IRRM-530; weight from 0.0129 to 0.0134g were irradiated in turn in Cd-lined outer irradiation channel A-3 and inner irradiation channel B-2 of NIRR-1 to check absolute neutron flux distribution. The irradiation time in inner channel B-2 lasted 30 minutes while in outer channel A-3 lasted 2 hours. A waiting period of 1140 seconds was observed for the irradiation in B-2 before a measurement of 60seconds was carried out for the first gamma-ray measurements at a distance of 17cm from the HPGe detector's end cap. After a day waiting of 76740seconds, the irradiated Au-Al foil at B-2 was re-measured at 2cm for 1800 seconds. The first measurement (S1) was done at 17cm geometry after a waiting time of 8 minutes while for second counting (S2) at 2 cm geometry, the delayed period was 75120 seconds. The measurement time was 600 seconds for the first count while 1800 seconds for the second count. The flux measurements of Φ_{fast}, Φ_{th}, and Φ_{epi} were performed following Eq. 8, 9, & 10 and results obtained are shown in Table 2.

Table 2: Nuclear Data Generated and Measured Thermal, Epithermal and Fast Neutron Fluxes

Irradiation Channel	B-2 Inner 1st	B-2 Inner 2nd	A-3 Outer 1st	A-3 Outer 2nd	B-2 Inner 1st	A-3 Outer 1st
Geometry (cm)	17	2	17	2	17	17
Saturated Factor	0.0053	0.0053	0.02117	0.02117	0.88899	0.99984
Decay Factor	0.9966	0.7961	0.99857	0.79995	0.24911	0.55645
Counting Factor	1.78E-03	5.33E-03	1.78E-03	5.33E-03	5.19E-01	5.19E-01
Pro-Isotope	^{197}Au	^{197}Au	^{197}Au	^{197}Au	^{197}Mg	^{24}Na
Measuring time (t_m)	600	1800	600	1800	600	600
Irradiation time (t_{irr})	1800	1800	7200	7200	1800	7200
E_γ (keV)	411.8		411.8	411.8	843.7	843.7
Cooling time (t_c)	1140	76740	480	75120	1140	480
Neutron Flux Measurements ($ncm^{-2}s^{-1}$)	**Thermal Flux (Φ_{th}) 4.75E+11**	**Thermal Flux (Φ_{th}) 5.04E+11**	**Epithermal Flux (Φ_{epi}) 3.96E+09**	**Epithermal Flux (Φ_{epi}) 4.48E+09**	**Fast Flux (Φ_{fast}) 9.15E+10**	**Fast Flux (Φ_{fast}) 1.08E+10**

In other to check the stability of neutron flux distribution of NIRR-1 irradiation channels, we determined the specific activity in A-1, A-3, B-2, B-3, and B-4 based on the nuclear reactions 1-5 above. For the measurement of flux stability, five Cu wires of weights 0.0987g to 0.1388g were irradiated in channels; A-1, A-3, B-2, B-3, and B-4 and two Au-0.1% Al foils of 0.1mm thick (IRRM-530), were irradiated in channels A-3 and B-2.

The Cu wires irradiation procedures in the five channels A-1, A-3, B-2, B-3, and B-4 are shown in Table 3 and the measurement at 17cm using GEM-30195 are shown in Table 3.

Table 3: Cu Wires Irradiation and Measurements Procedures in the Five Channels

Channels	Irradiation time (sec.)	Delayed time (sec)	Measured (seconds)
A-1	60	2100	600
A-3	300	660	300
B-2	60	2040	300
B-3	60	2040	300
B-4	120	1860	600

The irradiation of Au-0.1% Al foils A-3 was 300 seconds 120 seconds in B-2 and the measurements for first count at 17cm were 600 seconds both channels while second count at 2cm were 1800seconds both channels. The results of the specific activity in terms of nuclear reaction ^{27}Al (n, p) ^{27Mg}, ^{27}Al (n, α) ^{24Na}, and 197Au (n, γ) ^{198}Au are shown in Tables 4-6.

Table 4: Specific Activity Measurement in B-2 and A-3 using (n, p) and (n, α) Reactions

Channels	B-2 Inner 1st (17cm)	A-3 Outer 1st (17cm)	B-2 Inner 2nd (2cm)	A-3Outer2nd (2cm)
Sample ID	069M186	069M188	069M186	069M188
Wieght	0.0129	0.0134	0.0129	0.0134
Peak energy (KeV)	1014	1014	1368.6	1368.6
Irradiation time (sec)	1800	7200	1800	7200
Waiting time (sec)	1140	480	76740	75120
Measuring time (sec)	600	600	1800	1800
Decay Constant (λ)	0.00122119	0.00122119	1.28704E-05	1.28704E-05
Nuclear reaction	^{27}Al(n,p)^{27}Mg	^{27}Al(n,p)^{27}Mg	^{27}Al(n,α)^{24}Na	^{27}Al(n,α)^{24}Na
Specific Activity ($Bqkg^{-1}$)	**2163.72**	**253.55**	**13801.99**	**1945.25**

Table 5: Specific Activity Measurement in B-2 and A-3 using (n, p) Reactions

Channels	B-2 Inner 1st (17cm)	A-3 Outer 1st (17cm)
Sample ID	069M186	069M188
Wieght	0.0129	0.0134
Peak energy (KeV)	843	1014
Irradiation time (sec)	1800	7200
Waiting time (sec)	1140	480
Measuring time (sec)	600	600
Decay Constant (λ)	1.2E-03	1.2E-03
Nuclear reaction	$^{27}Al(n,p)^{27}Mg$	$^{27}Al(n,p)^{27}Mg$
Specific Activity (Bqkg^{-1})	**6384.74**	**748.99**

Table 6: Specific Activity Measurement in B-2 and A-3 using (n, γ) Reactions

Channels	B-2 Inner 1st (17cm)	A-3 Outer 1st (17cm)	B-2 Inner 2nd (2cm)	A-3 Outer 2nd (2cm)
Sample ID	069M186	069M188	069M186	069M188
Wieght	0.0129	0.0134	0.0129	0.0134
Peak energy (KeV)	411.8	411.8	411.8	411.8
Irradiation time (sec)	1800	7200	1800	7200
Waiting time (sec)	1140	480	76740	75120
Measuring time (sec)	600	600	1800	1800
Decay Constant (λ)	2.97068E-06	2.97131E-06	2.97131E-06	2.97131E-06
Nuclear reaction	$^{197}Au(n,\gamma)^{198}Au$	$^{197}Au(n,\gamma)^{198}Au$	$^{197}Au(n,\gamma)^{198}Au$	$^{197}Au(n,\gamma)^{198}Au$
Specific Activity (Bqkg^{-1})	**421037.5063**	**31840.74768**	**5714584.957**	**460734.7741**

The specific activity measurements for all channels; A-1, A-3, B-2, B-3, and B-4 with respect to the nuclear reaction $^{63}Cu\ (n, \gamma)\ ^{64Cu}$ are shown in Table 7.

Table 7: Specific Activity Measurements in A-1, A-3, B-2, B-3 and B-4 using (n, γ) Reaction

Channels	A-3 outer	B-2 Inner	B-3 Inner	B-4 Outer	A-1 Inner
Sample ID	069M163	069M167	069M171	069M165	069M169
Wieght	0.1389	0.1091	0.0988	0.1223	0.091
Peak energy (KeV)	1346	1346	1346	1346	1346
Irradiation time (sec)	300	60	60	120	60
Waiting time (sec)	660	2040	2040	1860	2100
Measuring time (sec)	600	600	600	600	600
Decay Constant (λ)	1.52E-05	1.52E-05	1.52E-05	1.52E-05	1.52E-05
Nuclear reaction	$^{63}Cu(n,\gamma)^{64}Cu$	$^{63}Cu(n,\gamma)^{64}Cu$	$^{63}Cu(n,\gamma)^{64}Cu$	$^{63}Cu(n,\gamma)^{64}Cu$	$^{63}Cu(n,\gamma)^{64}Cu$
Specific Activity (Bqkg^{-1})	**1870.41**	**40970.14**	**42453.39**	**20905.87**	**45214.85**

4. Results and Discussion

The average values of the neutron flux spectrum parameters measured in the first and second counts (17cm and 2cm) for Φ_{th} resulted to 4.89E+11 n/cm^{2}s in B-2 inner irradiation channel. This value confirmed very well with the recommended value of 5E+11n/cm^{2}s with uncertainty of 0.022% for inner channel of NIRR-1 on the operation control console. Due to the stability nature in flux distribution in NIRR-1, the Φ_{th} in A-1, B-3 were evaluated and was equal to that in B-2. However, since the flux in the inner channel doubles that in the outer channel, then the flux in B-4 outer channel was obtained to be 2.45E+11 n/cm^{2}s with uncertainty of 0.022%.

From the relationship in Eq. 5, making use of the generated nuclear data in Table 3, the Φ_{epi} in the inner channels A-1, B-2, and B-3 are obtained to be 2.55E+10 $ncm^{-2}s^{-1}$ while in the outer B-4 channel, the Φ_{epi} was 1.28E+10 $ncm^{-2}s^{-1}$. The measurement of the average value of Φ_{epi}, in the Cd-lined irradiation channel A-3 was 4.22E+09 n/cm^2s with uncertainty of 0.05%. The fast flux Φ_{fast} in the inner B-2 channel was 9.15E+10 n/cm^2s while the outer Cd-lined A-3 was 1.08E+10 n/cm^2s. These values tally very well with the thermal flux reading on the control console as shown in Fig. 1. These results indicate that neutron flux distributions have not been affected by the installation of Cd-liner in the outer channels A-3.

In theory, the specific activity ratios evaluation of inner-to-inner and outer-to-outer irradiation channels are calculated as follow:

$$A_{bare(inner)}^{Cu(B-2)} \approx A_{bare(inner)}^{Cu(B-3)} \approx A_{bare(inner)}^{Cu(A-1)}$$
$$A_{bare(outer)}^{Cu(B-4)} \approx A_{bare(outer)}^{Cu(A-3)} \quad (11)$$

$$\frac{A_{bare(inner)}^{Cu(B-2)}}{A_{bare(outer)}^{Cu(B-4)}} \approx \frac{\Phi_{th1}\sigma_{th} + \Phi_{epi1}I_0(\alpha)}{\Phi_{th2}\sigma_{th} + \Phi_{epi2}I_0(\alpha)}$$
$$\frac{A_{bare(inner)}^{Cu(B-2)}}{A_{bare(outer)}^{Cu(B-4)}} = \frac{\left[\Phi_{th2}\sigma_{th} + \Phi_{epi2}I_0(\alpha)\right]}{\Phi_{th2}\sigma_{th} + \Phi_{epi2}I_0(\alpha)} = 1 \quad (12)$$

where $\frac{\Phi_{th1}}{\Phi_{th2}} = 1$ and $\frac{\Phi_{epi1}}{\Phi_{epi2}} = 1$ obtained from Table 2 and $A_{bare(inner)}^{Cu(B-2)}$ = Specific activity of Cu in B-2

The experimental specific activity ratios, inner-to-inner (i.e., A-1/B-2, B-3/B-2, and A-1/B-3) were found to be 1.10 (0.01%), 1.03 (0.03%), and 1.06 (0.06%) respectively as shown in Table 8. Between the inner-to-outer, theoretical calculations shows that;

$$A_{bare(inner)}^{Cu(B-2)} \approx 2A_{bare(outer)}^{Cu(B-4)} \quad (13)$$

where $\frac{\Phi_{th1}}{\Phi_{th2}} = 2$ and $\frac{\Phi_{epi1}}{\Phi_{epi2}} = 2$ we have;

$$\frac{A_{bare(inner)}^{Cu(B-2)}}{A_{bare(outer)}^{Cu(B-4)}} \approx \frac{\Phi_{th1}\sigma_{th} + \Phi_{epi1}I_0(\alpha)}{\Phi_{th2}\sigma_{th} + \Phi_{epi2}I_0(\alpha)} \quad (14)$$

$$\frac{A_{bare(inner)}^{Cu(B-2)}}{A_{bare(outer)}^{Cu(B-4)}} = \frac{2\left[\Phi_{th2}\sigma_{th} + \Phi_{epi2}I_0(\alpha)\right]}{\Phi_{th2}\sigma_{th} + \Phi_{epi2}I_0(\alpha)} = 2 \quad (15)$$

From the experimental determination of specific activity ratios, inner-to-outer (A-1/B-4, B-2/B-4, and B-3/B-4) were determined to be 2.1 (0.01%), 1.9 (-0.01%) and 2.0 (0.001%) as shown in Table 8. Finally, between the inner-to-outer with Cd-lined A-1/A-3 measurements, the specific activity ratios was 22.17 while the outer-to-outer with Cd-lined B-4/A-3 was obtained to 11.18 as shown in Table 8.

Table 8: Specific activity ratios between irradiation channels of NIRR-1 for thermal, epithermal, and fast neutron reactions

Channel Relationship	Specific Activity Ratios	Theory Specific Activity Ratios
Inner-to-inner (A1/B2)	1.103604992	1
Inner-to-inner (B3/B2)	1.036203245	1
Inner-to-inner (A1/B3)	1.06504684	1
Inner-to-outer (A1/B4)	2.102782299	2
Inner-to-outer (B2/B4)	1.959743129	2
Inner-to-outer (B3/B4)	2.030692189	2
Inner-to-outer Cd-liner (A1/A3)	22.17380445	22
Outer-to-outer Cd-liner (B4/A3)	11.17717879	11

In theory, the inner-to-outer with Cd-lined and outer-to-outer with Cd-lined are estimation given as;

$$A_{bare(inner)}^{Cu(irradiation\ 'channel')} \approx 2A_{Cd(outer)}^{Cu(irradiation\ 'channel')}$$

$$(22.18)_{bare(inner)}^{Cu(irradiation\ 'channel')} \approx 2(11.18)_{Cd(outer)}^{Cu(irradiation\ 'channel')} \quad (16)$$

where $A_{Cd(outer)}^{Cu(irradiation\ 'channel')}$ =Specific activity ratio of Cd-lined (A-3)

These specific activity ratios values indicates that neutron flux distributions have not been affected by the installation of Cd-liner in the outer channel A-3 and the ratio of 2:1 for the inner-to-outer irradiation channels. The graphical interpretations of these results are shown in Figure 1-2.

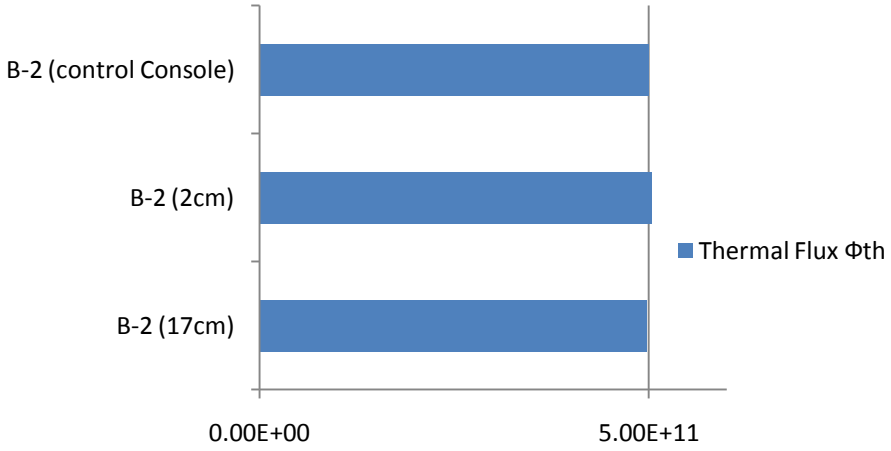

Figure 1: Thermal Neutron Flux Measurement of B-2 Inner Irradiation Channel of NIRR-1 at two different instances.

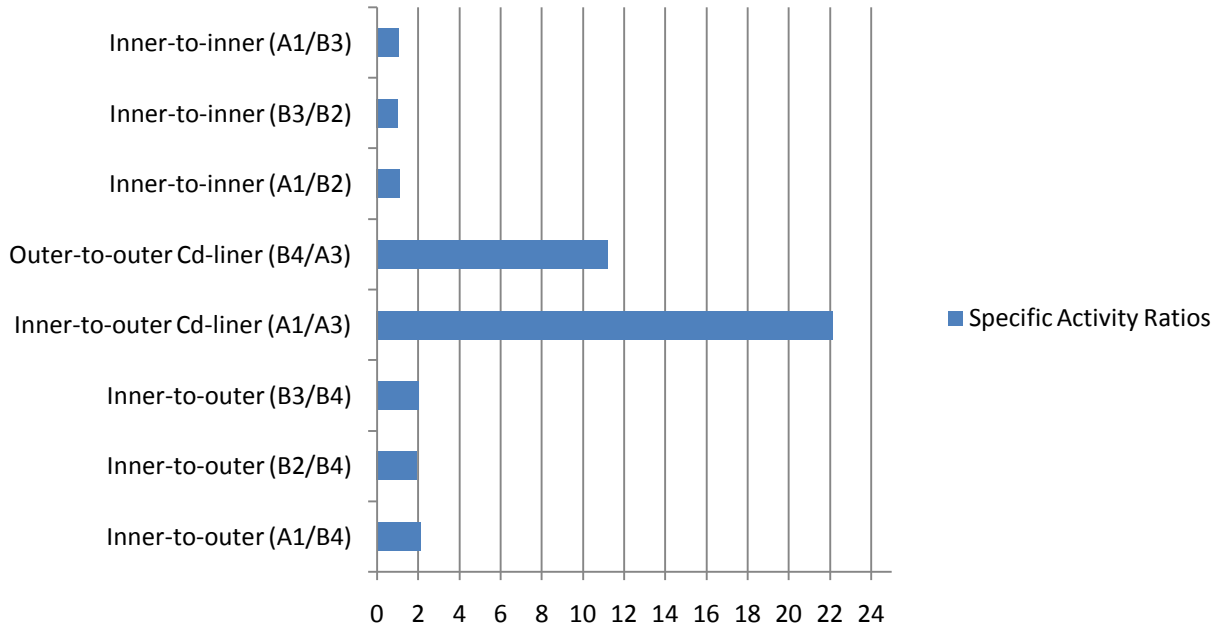

Figure 2: Channel Specific Activity Ratios

5. Conclusion

This work concludes that the operational routine in NAA analysis, it is sufficient to operate NIRR-1 at half power, which corresponds to a neutron flux of 5.0E+11 n/cm^2.s, in the inner irradiation channels. This confirmed the installation of Cd-lined in A-3 and has expand the margin of elemental investigation in all ramifications since during this steady state of operation at ½ power, the control rod is gradually withdrawn to compensate for reactivity loss due the large overall negative temperature coefficient of reactivity. Consequently, magnitude of the neutron flux remains constant during operation before and after the Cd-lined channel A-3. This work also confirmed the fact that the stability of the neutron flux is one of the hallmarks of NIRR-1 and similar facilities, which run on this same fuel loading for over 10 years. However, since the fuel is not modified at all for its entire core life time, the neutron spectrum in the irradiation channels does not change even when a Cd-lined was recently installed in the outer irradiation channel A-3 and the neutron flux is reproducible to within 1%. This therefore, allows convenient neutron activation analysis of all elements of interest in any of the channels A-1, A-3, B-2, B-3 and B-4 without the need to continually repeat the standardization measurements for all elements.

Acknowledgment

The authors thank CERT-Nigeria for the enabling environment and used of their facility for this research work.

References

Balogun G.I, Jonah S.A., Umar I.M., Measures aimed at enhancing safe operation of the Nigeria Research Reactor-1 (NIRR-1). In Book of Contributed Papers, International Conference on Operational Safety Performance in Nuclear Installations, 30 November – 2 December, 2005, IAEA, Vienna Austria, IAEA-CN-133/19, pg 93 – 96.

De Corte F., Dejaeger M., Hossain S. M., Vandenberghe D., De Wispelaere A., Van den Haute P. *A performance comparison of k0-based ENAA and NAA in the (K, Th, U) radiation dose rate assessment for the luminescence dating of sediments.* Journal of Radioanalytical and Nuclear Chemistry, Vol. 263, No. 3 (2005) 659.665

De Corte, F. The standardization of standardless NAA. Journal of Radio- analytical and Nuclear Chemistry (2001) 248 (1), 13–20.

De Corte, F., Problems and solutions in the standardization of reactor neutron activation analysis. Journal of Radio-analytical and Nuclear Chemistry (1992) 160 (1),63–75.

Jonah S.A, Umar I.M., Oladipo M.O.A, Balogun G.I., Adeyemo D.J., Standardization of NIRR-1 Irradiation and Counting Facilities for Instrumental Neutron Activation Analysis. Appld Rad. & Isotopes, 64, (2006), 818-822

Jonah S.A., Balogun G.I., Umar I.M., Mayaki M.C., Neutron spectrum parameters in irradiation channels of the Nigeria Research Reactor-1 (NIRR-1) for the *k0*NAA standardization. J. Radiaonal. Nucl. Chem.266, (2005), 83-88

Jonah S.A., Liaw J.R., Matos J.E., Monte Carlo simulation of core physics parameters of the Nigeria Research Reactor-1(NIRR-1). Annals Nucl. Energy 54, (2007), 953-957

Witkowska, E., Szczepaniak, K., Biziuk, M. Some applications of neutron activation analysis. Journal of Radioanalytical and Nuclear Chemistry (2005) 265 (1), 141–150.

Yavar A.R., Sarmani S.B., WoodA.K., Fadzil S.M., Radir M.H., Khoo K.S. Determination of fast neutron flux distribution in irradiation sites of the Malaysian Nuclear Agency research reactor. Journal of Applied Radiation and Isotopes 69 (2011) 762–767

Zhou Yongmao, IAEA-TECDOC-384 "Technology and Use of Low Power Research Reactors". Report of IAEA Consultants Meeting, Beijing, China 30 April – 3 May 1985, (1986) pg 89-98